Journal Pre-proof

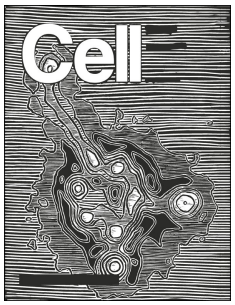

A single-dose intranasal ChAd vaccine protects upper and lower respiratory tracts against SARS-CoV-2

Ahmed O. Hassan, Natasha M. Kafai, Igor P. Dmitriev, Julie M. Fox, Brittany K. Smith, Ian B. Harvey, Rita E. Chen, Emma S. Winkler, Alex W. Wessel, James Brett Case, Elena Kashentseva, Broc T. McCune, Adam L. Bailey, Haiyan Zhao, Laura A. VanBlargan, Ya-Nan Dai, Meisheng Ma, Lucas J. Adams, Swathi Shrihari, Jonathan E. Danis, Lisa E. Gralinski, Yixuan J. Hou, Alexandra Schäfer, Arthur S. Kim, Shamus P. Keeler, Daniela Weiskopf, Ralph S. Baric, Michael J. Holtzman, Daved H. Fremont, David T. Curiel, Michael S. Diamond

PII: S0092-8674(20)31068-0

DOI: https://doi.org/10.1016/j.cell.2020.08.026

Reference: CELL 11573

To appear in: *Cell*

Received Date: 13 July 2020

Revised Date: 3 August 2020

Accepted Date: 14 August 2020

Please cite this article as: Hassan, A.O., Kafai, N.M., Dmitriev, I.P., Fox, J.M., Smith, B.K., Harvey, I.B., Chen, R.E., Winkler, E.S., Wessel, A.W., Case, J.B., Kashentseva, E., McCune, B.T., Bailey, A.L., Zhao, H., VanBlargan, L.A., Dai, Y.-N., Ma, M., Adams, L.J., Shrihari, S., Danis, J.E., Gralinski, L.E., Hou, Y.J., Schäfer, A., Kim, A.S., Keeler, S.P., Weiskopf, D., Baric, R.S., Holtzman, M.J., Fremont, D.H., Curiel, D.T., Diamond, M.S., A single-dose intranasal ChAd vaccine protects upper and lower respiratory tracts against SARS-CoV-2, *Cell* (2020), doi: https://doi.org/10.1016/j.cell.2020.08.026.

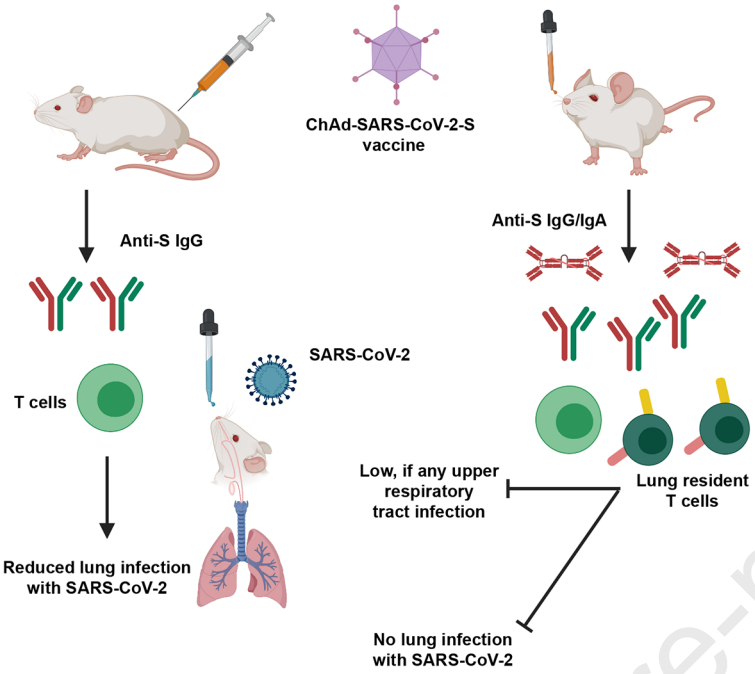

A single-dose intranasal ChAd vaccine protects upper and lower respiratory tracts against SARS-CoV-2

Ahmed O. Hassan[1], Natasha M. Kafai[1,3], Igor P. Dmitriev[2], Julie M. Fox[1], Brittany K. Smith[5], Ian B. Harvey[5], Rita E. Chen[1,3], Emma S. Winkler[1,3], Alex W. Wessel[1,3], James Brett Case[1], Elena Kashentseva[2], Broc T. McCune[1], Adam L. Bailey[3], Haiyan Zhao[3], Laura A. VanBlargan[1], Ya-Nan Dai[3], Meisheng Ma[3], Lucas J. Adams[3], Swathi Shrihari[1], Jonathan E. Danis[3], Lisa E. Gralinski[9], Yixuan J. Hou[9], Alexandra Schäfer[9], Arthur S. Kim[1,3], Shamus P. Keeler[6], Daniela Weiskopf[8], Ralph S. Baric[9,10], Michael J. Holtzman[1,6], Daved H. Fremont[3,5,7], David T. Curiel[2,7]*, and Michael S. Diamond[1,3,4,7]*‡

Department of Medicine[1], Radiation Oncology[2], Pathology & Immunology[3], Molecular Microbiology[4], Biochemistry and Molecular Biophysics[5], Washington University School of Medicine, St. Louis, MO 63110, USA. Division of Pulmonary and Critical Care Medicine[6], Washington University School of Medicine, St. Louis, MO 63110, USA. [7]The Andrew M. and Jane M. Bursky Center for Human Immunology & Immunotherapy Programs, Washington University School of Medicine, St. Louis, MO 63110, USA. [8]Center for Infectious Disease and Vaccine Research, La Jolla Institute for Immunology, La Jolla, CA 92037, USA. [9]Department of Epidemiology, [10]Department of Microbiology and Immunology, University of North Carolina at Chapel Hill, Chapel Hill, NC, USA

Corresponding authors: David T. Curiel (dcuriel@wustl.edu) and Michael S. Diamond, M.D., Ph.D. (diamond@wusm.wustl.edu)

‡ Lead Contact: Michael S. Diamond, M.D., Ph.D.

Figures: 7; Supplemental Figures:6

SUMMARY

The Coronavirus Disease 2019 pandemic has made deployment of an effective vaccine a global health priority. We evaluated the protective activity of a chimpanzee adenovirus-vectored vaccine encoding a pre-fusion stabilized spike protein (ChAd-SARS-CoV-2-S) in challenge studies with Severe Acute Respiratory Syndrome Coronavirus 2 (SARS-CoV-2) and mice expressing the human angiotensin-converting enzyme 2 receptor. Intramuscular dosing of ChAd-SARS-CoV-2-S induces robust systemic humoral and cell-mediated immune responses and protects against lung infection, inflammation, and pathology but does not confer sterilizing immunity, as evidenced by detection of viral RNA and induction of anti-nucleoprotein antibodies after SARS-CoV-2 challenge. In contrast, a single intranasal dose of ChAd-SARS-CoV-2-S induces high levels of neutralizing antibodies, promotes systemic and mucosal IgA and T cell responses, and virtually completely prevents SARS-CoV-2 infection in both the upper and lower respiratory tracts. Intranasal administration of ChAd-SARS-CoV-2-S is a candidate for preventing SARS-CoV-2 infection and transmission, and curtailing pandemic spread.

INTRODUCTION

Severe acute respiratory syndrome coronavirus 2 (SARS-CoV-2) is a positive-sense single-stranded RNA virus that was first isolated in late 2019 from patients with severe respiratory illness in Wuhan, China (Zhou et al., 2020b). SARS-CoV-2 is related to two other highly pathogenic respiratory viruses, SARS-CoV and Middle East respiratory syndrome coronavirus (MERS-CoV). SARS-CoV-2 infection results in a clinical syndrome, Coronavirus Disease 2019 (COVID-19) that can progress to respiratory failure (Guan et al., 2020) and also present with cardiac pathology, gastrointestinal disease, coagulopathy, and a hyperinflammatory syndrome (Cheung et al., 2020; Mao et al., 2020; Wichmann et al., 2020). The elderly, immunocompromised, and those with certain co-morbidities (*e.g*., obesity, diabetes, and hypertension) are at greatest risk of death from COVID-19 (Zhou et al., 2020a). Virtually all countries and territories have been affected with more than twenty million infections to date, hundreds of thousands of deaths, and a case-fatality rate estimated at ~4%. The extensive morbidity, mortality, and destabilizing socioeconomic consequences of COVID-19 highlight the urgent need for deployment of an effective SARS-CoV-2 vaccine to mitigate the severity of infection, curb transmission, end the pandemic, and prevent its return.

The SARS-CoV-2 RNA genome is approximately 30,000 nucleotides in length. The 5' two-thirds encode nonstructural proteins that enable genome replication and viral RNA synthesis. The remaining one-third encode structural proteins such as spike (S), envelope, membrane, and nucleoprotein (NP) that form the spherical virion, and accessory proteins that regulate cellular responses. The S protein forms homotrimeric spikes on the virion and engages the cell-surface receptor angiotensin-converting enzyme 2 (ACE2) to promote coronavirus entry into human cells (de Wit et al., 2016; Letko et al., 2020). The SARS-CoV and SARS-CoV-2 S proteins are cleaved sequentially during the entry process to yield S1 and S2 fragments, followed by further processing of S2 to yield a smaller S2' protein (Hoffmann et al., 2020). The S1 protein includes the receptor binding domain (RBD) and the S2 protein promotes membrane

fusion. The structure of a soluble, stabilized prefusion form of the SARS-CoV-2 S protein was solved by cryo-electron microscopy, revealing considerable similarity to the SARS-CoV S protein (Wrapp et al., 2020). This form of the S protein is recognized by potently neutralizing monoclonal antibodies (Cao et al., 2020; Pinto et al., 2020; Zost et al., 2020) and could serve as a promising vaccine target.

Release of the SARS-CoV-2 genome sequence immediate development of vaccine candidates that principally targeted the viral S protein (Burton and Walker, 2020). Multiple platforms have been developed to deliver the SARS-CoV-2 S protein including DNA plasmid, lipid nanoparticle encapsulated mRNA, inactivated virion, and viral-vectored vaccines (Graham, 2020). Several vaccines have entered clinical trials to evaluate safety, and some have advanced to trials assessing immunogenicity and efficacy. Most vaccines advanced to human testing without substantive efficacy data in animals (Diamond and Pierson, 2020). This circumstance occurred in part because vaccine design and development has outpaced the generation of accessible pre-clinical disease models of SARS-CoV-2 infection and pathogenesis.

Adenovirus (Ad)-based vaccines against coronaviruses have been evaluated previously. A single dose of a chimpanzee Ad-vectored vaccine encoding the S protein of MERS-CoV protected mice from infection (Munster et al., 2017), reduced virus shedding and enhanced survival in camels (Alharbi et al., 2019), and was safe and immunogenic in humans in a phase 1 clinical trial (Folegatti et al., 2020a). A human Ad-based vaccine expressing a MERS S1-CD40L fusion protein also was protective in mice (Hashem et al., 2019). An Ad-based SARS-CoV vaccine expressing the S protein prevented pneumonia in ferrets after challenge and was highly immunogenic in rhesus macaques (Kobinger et al., 2007). A chimpanzee Ad vector (Y25, a simian Ad-23 (Dicks et al., 2012)) encoding the SARS-CoV-2 S protein (ChAdOx1 nCoV-19) is currently under evaluation in humans as a single intramuscular injection (NCT04324606). Preliminary analysis suggests this vaccine protects against lung infection and pneumonia but

not against upper respiratory tract infection and virus shedding (https://doi.org/10.1101/2020.05.13.093195).

Here, we develop a different chimpanzee Ad (simian Ad-36)-based SARS-CoV-2 vaccine (ChAd-SARS-CoV-2-S) encoding a pre-fusion stabilized spike (S) protein after introducing two proline substitutions in the S2 subunit (Pallesen et al., 2017). Intramuscular administration of ChAd-SARS-CoV-2-S induced robust systemic humoral and cell-mediated immune responses. One or two vaccine doses protected against lung infection, inflammation, and pathology after SARS-CoV-2 challenge of mice that transiently express the human ACE2 (hACE2) receptor. Despite the induction of high levels of neutralizing antibody, neither dosing regimen completely protected against SARS-CoV-2 infection, as substantial levels of viral RNA were still detected in the lung. In comparison, a single intranasal dose of ChAd-SARS-CoV-2-S induced high levels of neutralizing antibody and anti-SARS-CoV-2 IgA, and conferred virtually complete protection against infection in both the upper and lower respiratory tracts in mice expressing hACE2 receptor after adenoviral vector delivery or as a transgene. Thus, ChAd-SARS-CoV-2-S has the potential to control infection at the site of inoculation, which should prevent both virus-induced disease and transmission.

RESULTS

Chimpanzee Ad-vectored vaccine induces robust antibody responses against SARS-CoV-2. We constructed two replication-incompetent ChAd vectors based on a simian Ad-36 virus. The ChAd-SARS-CoV-2-S vector encodes the full-length, codon optimized sequence of SARS-CoV-2 S protein as a transgene including the ectodomain, transmembrane domain, and cytoplasmic domain (GenBank: QJQ84760.1) and is stabilized in pre-fusion form by two proline substitutions at residues K986 and V987 (Pallesen et al., 2017; Wrapp et al., 2020). The ChAd-control has no transgene. The S protein transgene is controlled transcriptionally by a cytomegalovirus promoter. To make the vector replication-incompetent and enhance packaging capacity, we replaced the E1A/B genes and introduced a deletion in the E3B gene, respectively (**Fig 1A**). To confirm that the S protein was expressed and antigenically intact, we transduced 293T cells and confirmed binding of a panel of 22 neutralizing monoclonal antibodies against the S protein by flow cytometry (**Fig 1B**).

To assess the immunogenicity of ChAd-SARS-CoV-2-S, groups of 4-week-old BALB/c mice were immunized by intramuscular inoculation with 10^{10} virus particles of ChAd-SARS-CoV-2-S or ChAd-control. Some mice received a booster dose four weeks later. Serum samples were collected 21 days after primary or booster immunization (**Fig 1C**), and IgG responses against purified S and RBD proteins were evaluated by ELISA. Whereas ChAd-SARS-CoV-2-S induced high levels of S- and RBD-specific IgG, low, if any levels were detected in the ChAd-control-immunized mice (**Fig 1D**). However, intramuscular injection of ChAd-SARS-CoV-2-S failed to induce S- or RBD-specific IgA in serum (**Fig 1E**). We next functionally characterized serum antibody responses by assaying neutralization of infectious SARS-CoV-2 using a focus-reduction neutralization test (FRNT) (Case et al., 2020). As expected, serum from ChAd-control-immunized mice did not inhibit SARS-CoV-2 infection after primary immunization or boosting. In contrast, serum from ChAd-SARS-CoV-2-S vaccinated animals neutralized SARS-CoV-2

infection, and boosting enhanced this inhibitory activity (geometric mean titers (GMT) of 1/240 and 1/719, respectively) (**Fig 1F and S1A-B**).

Vaccine-induced memory CD8$^+$ T cell and antigen specific B cell responses. Because optimal vaccine immunity is often comprised of both humoral and cellular responses (Slifka and Amanna, 2014), we measured the levels of SARS-CoV-2-specific CD4$^+$ and CD8$^+$ T cells after vaccination. Four-week old BALB/c mice were immunized with ChAd-SARS-CoV-2-S or ChAd-control and boosted three weeks later. To assess the vaccine-induced SARS-CoV-2-specific CD4$^+$ and CD8$^+$ T cell responses, splenocytes were harvested one week after boosting and stimulated *ex vivo* with a pool of 253 overlapping 15-mer S peptides (**Table S1**). Subsequently, quantification of intracellular IFNγ and granzyme B expression was determined by flow cytometry. After peptide re-stimulation *ex vivo*, splenic CD8$^+$ T cells expressed IFNγ and both splenic CD4$^+$ and CD8$^+$ T cells expressed granzyme B in mice immunized with ChAd-SARS-CoV-2-S but not the ChAd-control vector (**Fig 1G-H and S2**). To assess the antigen-specific B cell responses, splenocytes were harvested and subjected to an ELISPOT analysis with S protein. The ChAd-SARS-CoV-2-S vaccine induced S protein-specific IgG antibody-secreting cells in the spleen whereas the control vaccine did not (**Fig 1I**).

To assess whether intramuscular vaccination could induce mucosal immune responses in the lungs, mice were immunized with either ChAd-SARS-CoV-2-S or ChAd-control and boosted similarly four weeks later. Lungs were harvested one-week post-boosting, and T cells were analyzed by flow cytometry. Notably, we failed to detect an increase in IFNγ or granzyme B producing CD8$^+$ T cells in the lungs of ChAd-SARS-CoV-2-S vaccinated mice after re-stimulation *ex vivo* with a pool of S peptides (**Fig 1J**) or CD103$^+$CD69$^+$CD8$^+$ cells that could represent lung resident memory T cells (**Fig 1K**). In the spleen, we also failed to detect antibody-secreting plasma cells producing IgA against the S protein after immunization with ChAd-SARS-CoV-2-S (**Fig 1L**). Moreover, we detected low S-specific IgG and no S-specific IgA

or RBD-specific IgG or IgA antibodies in bronchoalveolar lavage (BAL) fluid of immunized mice (**Fig 1M-N**). Thus, while intramuscular vaccination with ChAd-SARS-CoV-2-S produced strong systemic adaptive immune responses against SARS-CoV-2, it induced little, if any, mucosal immune response.

Intramuscular immunization with ChAd-SARS-CoV-2-S vaccine protects against SARS-CoV-2 infection in the lung. We tested the protective activity of the ChAd vaccine in a recently developed SARS-CoV-2 infection model wherein BALB/c mice express hACE2 in the lung after intranasal delivery of a vectored human Ad (Hu-Ad5-hACE2) (Hassan et al., 2020). Endogenous mouse ACE2 does not support viral entry (Letko et al., 2020), and this system enables productive SARS-CoV-2 infection in the mouse lung. Four-week-old BALB/c mice first were immunized via an intramuscular route with ChAd-control or ChAd-SARS-CoV-2-S vaccines. Approximately thirty days later, mice were administered 10^8 plaque-forming units (PFU) of Hu-Ad5-hACE2 and anti-Ifnar1 monoclonal antibody (mAb) via intranasal and intraperitoneal routes, respectively. We also administered a single dose of anti-Ifnar1 mAb to -enhance lung pathogenesis in this model (Hassan et al., 2020). We confirmed the absence of cross-immunity between the ChAd and the Hu-Ad5 vector. Serum from ChAd-immunized mice did not neutralize Hu-Ad5 infection (**Fig S3A-B**).

Five days after Hu-Ad5-hACE2 transduction, mice were challenged via intranasal route with 4 x 10^5 focus-forming units (FFU) of SARS-CoV-2 (**Fig 2A**). At 4 days post-infection (dpi), the peak of viral burden in this model (Hassan et al., 2020), mice were euthanized, and lungs, spleen, and heart were harvested for viral burden and cytokine analysis. Notably, there was no detectable infectious virus in the lungs of mice immunized with ChAd-SARS-CoV-2-S as determined by plaque assay, whereas high levels were present in mice vaccinated with ChAd-control (**Fig 2B**). Using primers that target a sequence within the N gene, we also detected no measurable genomic or subgenomic viral RNA in the heart and spleen and lower levels of viral RNA in the lungs of ChAd-SARS-CoV-2-S vaccinated animals compared to mice receiving the

ChAd-control vector (**Fig 2C**). *In situ* hybridization staining for viral RNA in lungs harvested at 4 dpi revealed a substantial decrease of SARS-CoV-2 RNA in pneumocytes of animals immunized with ChAd-SARS-CoV-2-S compared to the ChAd-control (**Fig 2D**). A subset of immunized animals was euthanized at 8 dpi, and tissues were harvested for evaluation. At this time point, viral RNA levels again were lower or absent in the lung and spleen of ChAd-SARS-CoV-2-S immunized mice compared to the control ChAd vector (**Fig 2C**). Collectively, these data indicate that a single intramuscular immunization with ChAd-SARS-CoV-2-S results in markedly reduced, but not abrogated, SARS-CoV-2 infection in the lungs of challenged mice.

We next assessed the effect of the vaccine on lung inflammation and disease. Several proinflammatory cytokines and chemokine mRNA levels were lower in the lung tissues of animals immunized with ChAd-SARS-CoV-2-S compared to ChAd-control including *CXCL10*, *IL1β*, *IL6, CCL5, IFNβ,* and *IFNλ* (**Fig 2E**). Moreover, mice immunized with ChAd-control vaccine and challenged with SARS-CoV-2 showed evidence of viral pneumonia characterized by immune cell accumulation in perivascular and alveolar locations, vascular congestion, and interstitial edema. In contrast, animals immunized with ChAd-SARS-CoV-2-S showed a marked attenuation of the inflammatory response in the lung that develops in the ChAd-control-immunized mice (**Fig 3**). Thus, immunization with Ch-Ad-SARS-CoV-2 decreases both viral infection and the consequent lung inflammation and injury associated with SARS-CoV-2 infection.

We then assessed for improved protection using a prime-boost vaccine regimen. BALB/c mice were immunized via an intramuscular route with ChAd-control or ChAd-SARS-CoV-2-S and received a homologous booster dose four weeks later. At day 29 post-boost, mice were treated with a single dose of anti-Ifnar1 antibody followed by Hu-Ad5-hACE2 and then challenged with SARS-CoV-2 five days later. As expected, the prime-boost regimen protected against SARS-CoV-2 challenge with no infectious virus detected in the lungs (**Fig 2F**). Although marked reductions of viral RNA in the lung, spleen, and heart were detected at 4 dpi, residual

levels of viral RNA still were present suggesting protection was not complete, even after boosting (**Fig 2G**).

A single intranasal immunization with ChAd-SARS-CoV-2-S induces protective immunity against SARS-CoV-2 in mice expressing hACE2 delivered by an adenoviral vector. Mucosal immunization through the nasopharyngeal route can elicit local immune responses including secretory IgA antibodies that confer protection at or near the site of inoculation of respiratory pathogens (Neutra and Kozlowski, 2006). To assess the immunogenicity and protective efficacy of mucosal vaccination, five-week old BALB/c mice were inoculated via intranasal route with 10^{10} viral particles of ChAd-control or ChAd-SARS-CoV-2-S (**Fig 4A**). Serum samples were collected at four weeks post-immunization to evaluate humoral immune responses. Intranasal immunization of ChAd-SARS-CoV-2-S but not ChAd-control induced high levels of S- and RBD-specific IgG and IgA (**Fig 4B-C**) and SARS-CoV-2 neutralizing antibodies (GMT of 1/1,574) in serum (**Fig 4D and S4A**). Antibodies from mice immunized with ChAd-SARS-CoV-2-S equivalently neutralized a recombinant, luciferase-expressing variant of SARS-CoV-2 encoding a D614G mutation in the S protein (**Fig S4B**); this finding is important, because many circulating viruses contain this substitution, which is associated with greater infectivity in cell culture (Korber et al., 2020). We also assessed the SARS-CoV-2-specific antibody responses in BAL fluid of immunized mice. BAL fluid from ChAd-SARS-CoV-2-S but not ChAd-control vaccinated mice showed high levels of S- and RBD-specific IgG and IgA antibodies (**Fig 4E-F**) including those with neutralizing activity (**Fig 4G and S4C**).

To assess T cell responses activated via mucosal immunization, mice were vaccinated via intranasal route with either ChAd-SARS-CoV-2-S or ChAd-control and boosted similarly four weeks later. Lungs were harvested one-week post-boosting, and T cells were analyzed by flow cytometry. Re-stimulation *ex vivo* with a pool of S peptides resulted in a marked increase in IFNγ and granzyme B producing $CD8^+$ T cells in the lungs of mice that received the ChAd-

SARS-CoV-2-S vaccine (**Fig 4H**). Specifically, a population of IFNγ-secreting, antigen-specific $CD103^+CD69^+CD8^+$ T cells in the lung was identified (**Fig 4I**) which is phenotypically consistent with vaccine-induced resident memory T cells (Takamura, 2017). In the spleen, we detected antibody-secreting plasma cells producing IgA or IgG against the S protein after intranasal immunization with ChAd-SARS-CoV-2-S (**Fig 4J**). Of note, we observed an ~-5-fold higher frequency of B cells secreting anti-S IgA than IgG.

We evaluated the protective efficacy of the ChAd vaccine after single-dose intranasal immunization. At day 30 post-vaccination, mice were administered 10^8 PFU of Hu-Ad5-hACE2 and anti-Ifnar1 mAb as described above. Five days later, mice were challenged with 4 x 10^5 FFU of SARS-CoV-2. At 4 and 8 dpi, lungs, spleen, heart, nasal turbinates, and nasal washes were harvested and assessed for viral burden. Intranasal delivery of the ChAd-SARS-CoV-2-S vaccine demonstrated remarkable protective efficacy as judged by an absence of infectious virus in the lungs (**Fig 5A**) and almost no measurable viral RNA in the lung, spleen, heart, nasal turbinates, or nasal washes, as determined with subgenomic/genomic (N gene) or genomic only (ORF1a gene) TaqMan probes (**Fig 5B and S4D**). The very low viral RNA levels in the lung and nasal turbinates at 4 dpi may reflect the input, non-replicating virus, as similar amounts were measured at this time point in C57BL/6 mice lacking hACE2 receptor expression (Hassan et al., 2020). Cytokine and chemokine mRNA levels in lung homogenates also were substantially lower in mice immunized with the ChAd-SARS-CoV-2-S than the ChAd-control vaccine (**Fig 5C**), with residual expression likely due to the human Ad vector hACE2 delivery system. Finally, histopathological analysis of lung tissues from animals vaccinated with ChAd-SARS-CoV-2-S by intranasal route and challenged with SARS-CoV-2 showed minimal, if any, perivascular and alveolar infiltrates at 8 dpi compared to the extensive inflammation observed in ChAd-control vaccinated animals (**Fig 5D**).

To begin to determine if sterilizing immunity might be achieved with intranasal delivery of ChAd-SARS-CoV-2-S, we measured anti-NP antibodies at 8 dpi and compared them to

responses from 5 days before SARS-CoV-2 infection. Because the NP gene is absent from the vaccine vector, induction of humoral immune responses against NP after SARS-CoV-2 exposure (Ni et al., 2020) suggests viral protein translation and active infection. After SARS-CoV-2 challenge, anti-NP antibody responses were detected in ChAd-control mice vaccinated by an intranasal route or ChAd-control and ChAd-SARS-CoV-2-S mice vaccinated by an intramuscular route (**Fig 5E and S1C**). Remarkably, none of the mice immunized with ChAd-SARS-CoV-2-S via an intranasal route showed significant increases in anti-NP antibody responses after SARS-CoV-2 infection (**Fig 5E and S5**). Combined with our virological analyses, these data suggest that a single intranasal immunization of ChAd-SARS-CoV-2-S induces robust mucosal immunity, which prevents SARS-CoV-2 infection in the upper and lower respiratory tracts of mice expressing the hACE2 receptor.

A single intranasal immunization with ChAd-SARS-CoV-2-S prevents SARS-CoV-2 infection in the upper and lower respiratory tracts of hACE2 transgenic mice. Recently, we and others established a more stringent, lethal SARS-CoV-2 challenge model (Rathnasinghe et al., 2020; Winkler et al., 2020) in transgenic C57BL/6 mice that have eight inserted copies of the *hACE2* gene driven by the K18 cytokeratin epithelial cell promoter (McCray et al., 2007). Within one week of SARS-CoV-2 inoculation by an intranasal route, K18-hACE2 mice develop severe lung infection and inflammation, immune cell infiltration, and compromised respiratory function that results in death. As an independent test of the efficacy of intranasal administration of ChAd-SARS-CoV-2-S, we assessed its immunogenicity and protective efficacy in K18-hACE2 mice.

Four-week old K18-hACE2 mice were inoculated via an intranasal route with 10^{10} viral particles of ChAd-control or ChAd-SARS-CoV-2-S (**Fig 6A**). Serum samples were collected at four weeks post-immunization, and humoral immune responses were evaluated. Intranasal immunization of ChAd-SARS-CoV-2-S but not ChAd-control induced high levels of S- and RBD-specific IgG and IgA (**Fig 6B-C**) and neutralizing antibodies (GMT of 1/1,424) in serum (**Fig 6D**

289 **and S6**). At day 30 post-vaccination, K18-hACE2 mice were challenged via an intranasal route
290 with 10^3 FFU of SARS-CoV-2. At 4 dpi, lungs, spleen, heart, nasal turbinates, and nasal washes
291 were harvested and assessed for viral burden. Similar to that seen in BALB/c mice transiently
292 expressing hACE2, intranasal immunization of ChAd-SARS-CoV-2-S conferred remarkable
293 protection as judged by an absence of infectious virus in the lungs (**Fig 6E**), no measurable viral
294 subgenomic/genomic RNA in the lungs or hearts, and very low levels of viral RNA in the nasal
295 turbinates or washes (**Fig 6F**). Consistent with these results, after SARS-CoV-2 challenge, we
296 observed no induction of cytokine and chemokine mRNA (*e.g.*, CCL2, CXCL1, CXCL10,
297 CXCL11, IL6, IFNβ, and IFNλ) in the lung homogenates of ChAd-SARS-CoV-2-S-immunized
298 compared to naïve mice, whereas ChAd-control vaccinated mice sustained high levels (**Fig 6G**).
299 Collectively, these data suggest that a single intranasal immunization of ChAd-SARS-CoV-2-S
300 induces robust systemic and mucosal immunity that blocks SARS-CoV-2 infection in the upper
301 and lower respiratory tract of highly susceptible K18-hACE2 transgenic mice.
302

DISCUSSION

In this study, we evaluated intramuscular and intranasal administration of a replication-incompetent ChAd vector as a vaccine platforms for SARS-CoV-2. Single dose immunization of a stabilized S protein-based vaccine via an intramuscular route induced S- and RBD-specific binding as well as neutralizing antibodies. Vaccination with one or two doses protected mice expressing human ACE2 against SARS-CoV-2 challenge, as evidenced by an absence of infectious virus in the lungs and substantially reduced viral RNA levels in lungs and other organs. Mice immunized with ChAd-SARS-CoV-2-S also showed markedly reduced if not absent lung pathology, lung inflammation, and evidence of pneumonia compared to the control ChAd vaccine. However, intramuscular vaccination of ChAd-SARS-CoV-2-S did not induce IgA responses or confer sterilizing immunity, as evidenced by detectable viral RNA levels in the lung and induction of anti-NP antibody responses. Mice immunized with a single dose of the ChAd-SARS-CoV-2-S via an intranasal route also were protected against SARS-CoV-2 challenge. Intranasal vaccination, however, generated robust IgA and neutralizing antibody responses that likely protected against both upper and lower respiratory tract SARS-CoV-2 infection and inhibited infection of both wild-type and D614G variant viruses. The very low levels of genomic viral RNA in upper airway tissues and absence of serological response to NP in the context of challenge strongly suggests that at least some animals receiving a single intranasal dose of ChAd-SARS-CoV-2-S likely achieved sterilizing immunity.

Although several vaccine candidates (*e.g.*, lipid-encapsulated mRNA, DNA, inactivated, and viral-vectored) rapidly advanced to human clinical trials in an expedited effort to control the pandemic (Amanat and Krammer, 2020), few studies have demonstrated efficacy in pre-clinical models. Rhesus macaques immunized with two or three doses of a DNA plasmid vaccine encoding full-length SARS-CoV-2 S protein induced neutralizing antibody in sera and reduced viral burden in BAL and nasal mucosa fluids (Yu et al., 2020). Three immunizations over two weeks with purified, inactivated SARS-CoV-2 induced neutralizing antibodies, and depending on

329 the dose administered provided partial or complete protection against infection and viral
330 pneumonia in rhesus macaques (Gao et al., 2020). Finally, two intramuscular doses of a lipid
331 encapsulated mRNA-based vaccine against S protected against SARS-CoV-2 infection in nasal
332 swabs and BAL fluid of rhesus macaques (Corbett et al., 2020). One limitation of these
333 challenge models is that rhesus macaques develop lower viral burden and mild interstitial
334 pneumonia after SARS-CoV-2 infection compared to some humans and other non-human
335 primate species (Chandrashekar et al., 2020; Munster et al., 2020). Our study in hACE2-
336 expressing mice show that a single intramuscular or intranasal dose of ChAd-SARS-CoV-2-S
337 vaccine confers substantial and possibly complete protection against viral replication,
338 inflammation, and lung disease.

339 Our approach supports the use of non-human Ad-vectored vaccines against emerging
340 RNA viruses including SARS-CoV-2. Previously, we showed the efficacy of single-dose or two-
341 dose regimens of a gorilla Ad encoding the prM-E genes of Zika virus (ZIKV) in several mouse
342 challenge models including in the context of pregnancy (Hassan et al., 2019). Others have
343 evaluated ChAd or rhesus macaque Ad vaccine candidates against ZIKV and shown efficacy in
344 mice and non-human primates (Abbink et al., 2016; López-Camacho et al., 2018). A different
345 ChAd encoding the wild-type SARS-CoV-2 S protein (ChAdOx1) is currently in clinical trials in
346 humans (NCT04324606), and a phase 1/2 trial showed neutralizing antibody responses against
347 SARS-CoV-2 in 91% and 100% participants after one or two-dose immunization regimens
348 (Folegatti et al., 2020b). Studies in rhesus macaques with ChAdOx1 suggest that a single
349 intramuscular dose protects against infection in the lung but not in the upper respiratory tract
350 (https://www.biorxiv.org/content/10.1101/2020.05.13.093195v1). None of the vaccines
351 evaluated against SARS-CoV-2 has shown evidence of immune enhancement in any pre-
352 clinical or clinical study, which has been a theoretical risk based on studies with other human
353 and animal coronaviruses (de Alwis et al., 2020; Diamond and Pierson, 2020). Indeed, and in
354 contrast to data with SARS-CoV vaccines or antibodies (Bolles et al., 2011; Liu et al., 2019;

Weingartl et al., 2004), we did not observe enhanced infection, immunopathology, or disease in animals immunized with ChAd encoding SARS-CoV-2 S proteins or administered passively transferred monoclonal antibodies (Alsoussi et al., 2020; Hassan et al., 2020).

ChAd-SARS-CoV-2-S induced SARS-CoV-2 specific $CD8^+$ T cell responses including a high percentage and number of IFNγ and granzyme expressing cells after *ex vivo* S protein peptide restimulation. The induction of $CD8^+$ T cell responses by the ChAd-SARS-CoV-2-S vaccine is consistent with reports with other simian Ad vectors (Douglas et al., 2010; Hodgson et al., 2015; Reyes-Sandoval et al., 2010). ChAd vaccine vectors not only overcome issues of pre-existing immunity against human adenoviruses but also have immunological advantages because they do not induce exhausted T cell responses (Penaloza-MacMaster et al., 2013).

A single intranasal dose of ChAd-SARS-CoV-2-S conferred superior immunity against SARS-CoV-2 challenge, more so than one or two intramuscular immunizations of the same vaccine and dose (**Fig 7**). Additionally, one intranasal dose of ChAd-SARS-CoV-2-S prevented upper and lower respiratory tract infection and inflammation by SARS-CoV-2 in highly susceptible K18-hACE2 transgenic mice (Rathnasinghe et al., 2020; Winkler et al., 2020). Given that the serum neutralizing antibody responses were comparable, we hypothesize the greater protection observed after intranasal delivery was because of the mucosal immune responses generated. Indeed, high levels of anti-SARS-CoV-2 IgA were detected in serum and lung, and B cells secreting IgA were detected in the spleen only in mice vaccinated via an intranasal route. Moreover, intranasal but not intramuscular vaccination induced SARS-CoV-2-specific $CD8^+$ T cells in the lung including $CD103^+CD69^+$ cells, which are likely of a resident memory phenotype. Future antibody passive transfer and T cell depletion studies can assess the relative contribution of each immune arm to protection and establish more precisely the mechanistic basis for the enhanced protection conferred by intranasal delivery of ChAd-SARS-CoV-2-S.

To our knowledge, none of the SARS-CoV-2 vaccine platforms currently in clinical trials use an intranasal delivery approach. There has been great interest in using intranasal delivery

for influenza A virus vaccines because of their ability to elicit local humoral and cellular immune responses (Calzas and Chevalier, 2019). Indeed, sterilizing immunity to influenza A virus re-infection requires local adaptive immune responses in the lung, which is optimally induced by intranasal and not intramuscular inoculation (Dutta et al., 2016; Laurie et al., 2010). While there are concerns with administering live-attenuated viral vaccines via an intranasal route, subunit-based or replication-incompetent vectored vaccines are promising for generating mucosal immunity in a safer manner, especially given advances in formulation (Yusuf and Kett, 2017).

Limitations of study. Although a single intranasal administration of ChAd-SARS-CoV-2-S protected against SARS-CoV-2 replication in lungs, we note some limitations in our study. We performed most challenge studies in mice transduced with hACE2 using a human Ad5 vector, which could be complicated by vector immunity. Notwithstanding this possibility, we confirmed an absence of heterologous neutralizing serum antibody induced by one or two doses of ChAd vector against the Hu-Ad5 and more importantly, detected high levels of SARS-CoV-2 infection in the ChAd-control vaccinated mice after challenge. Moreover, we reproduced the level of protection by ChAd-SARS-CoV-2-S in K18-hACE2 transgenic mice. Immunization and challenge studies with non-human primates are planned to confirm the extent of protective mucosal immunity conferred by ChAd-SARS-CoV-2-S in mice and expand upon our understanding of how the route of inoculation impacts vaccine-mediated protection. Moreover, studies in humans are needed to assess for cross-immunity between the ChAd vector (simian Ad-36) and adenoviruses circulating in humans. Although we expect this will be much less than that observed with Hu-Ad5 vaccine vectors (Zhu et al., 2020), low levels of pre-existing immunity against simian adenoviruses could affect vaccine efficacy in selected populations with non-human primate exposures (*e.g.*, zoo workers, veterinarians, and laboratory workers at primate centers). Finally, studies must be conducted to monitor immune responses over time after intranasal vaccination with ChAd-SARS-CoV-2-S to establish the durability of the protective response.

In summary, our studies establish that immunization with ChAd-SARS-CoV-2-S induces both neutralizing antibody and antigen-specific $CD8^+$ T cell responses. While a single intramuscular immunization of ChAd-SARS-CoV-2-S confers protection against SARS-CoV-2 infection and inflammation in the lungs, intranasal delivery of ChAd-SARS-CoV-2-S induces mucosal immunity, provides superior protection, and possibly promotes sterilizing immunity, at least in mice that transiently or stably express the hACE2 receptor. We suggest that intranasal delivery of ChAd-SARS-CoV-2-S is a promising platform for preventing SARS-CoV-2 infection, disease, and upper airway transmission, and thus warrants clinical evaluation in humans.

MAIN FIGURE LEGENDS

Figure 1. Immunogenicity of ChAd-SARS-CoV-2-S. A. Diagram of transgene cassettes: ChAd-control has no transgene insert; ChAd-SARS-CoV-2-S encodes for SARS-CoV-2 S protein with the two indicated proline mutations. **B**. Binding of ChAd-SARS-CoV-2-S transduced 293 cells with anti-S mAbs. (*Left*) Summary: +, ++, +++, - indicate < 25%, 25-50%, > 50%, and no binding, respectively. MFI, mean fluorescence intensity. (*Right*) Representative flow cytometry histograms of two experiments. **C-F**. Four-week old female BALB/c mice were immunized via intramuscular route with ChAd-control or ChAd-SARS-CoV-2-S and boosted four weeks later. Antibody responses in sera of immunized mice at day 21 after priming or boosting were evaluated. An ELISA measured anti-S and RBD IgG and IgA levels (**D-E**), and an FRNT determined neutralization activity (**F**). Data are pooled from two experiments (n = 15 to 30). **G-H.** Cell-mediated responses were analyzed at day 7 post-booster immunization after re-stimulation with an S protein peptide pool (**Table S1**). Splenocytes were assayed for IFNγ and granzyme B expression in $CD8^+$ T cells and granzyme B only in $CD4^+$ T cells by flow cytometry (**G**). A summary of frequencies and numbers of positive cell populations is shown in **H** (n = 5). Bars indicate median values, and dotted lines are the limit of detection (LOD) of the assays. **I**. Spleens were harvested at 7 days post-boost, and SARS-CoV-2 spike-specific IgG+ antibody-secreting cells (ASC) frequency was measured by ELISPOT. $CD8^+$ T cells in the lung were assayed for IFNγ and granzyme B expression by flow cytometry after re-stimulation with an S protein peptide pool (**J**). Lung $CD8^+$ T cells also were assayed for expression of CD69 and CD103 (**K**). **L**. Spleens were harvested at 7 days post-boosting, and SARS-CoV-2 spike-specific IgA^+ antibody-secreting cells (ASC) frequency was measured by ELISPOT. **M-N.** SARS-CoV-2 S- and RBD-specific IgG and IgA levels in BAL fluid were determined by ELISA. Bars and columns show median values, and dotted lines indicate the limit of detection (LOD) of the

assays. For **D, F, H, I, and J**: Mann-Whitney test: *, $P < 0.05$; **, $P < 0.01$; ***, $P < 0.001$; **** $P < 0.0001$; ns, not significant. **See Figure S1, Figure S2, Figure S3, and Table S1**.

Figure 2. Protective efficacy of intramuscularly delivered ChAd-SARS-CoV-2-S against SARS-CoV-2 infection. A. Scheme of vaccination and challenge. Four-week-old BALB/c female mice were immunized ChAd-control or ChAd-SARS-CoV-2-S. Some mice received a booster dose of the homologous vaccine. On day 35 post-immunization, mice were challenged with SARS-CoV-2 as follows: animals were treated with anti-Ifnar1 mAb and transduced with Hu-AdV5-hACE2 via an intranasal route one day later. Five days later, mice were challenged with 4 x 10^5 focus-forming units (FFU) of SARS-CoV-2 via the intranasal route. **B-C.** Tissues were harvested at 4 and 8 dpi for analysis. Infectious virus in the lung was measured by plaque assay (**B**) and viral RNA levels were measured in the lung, spleen and heart at 4 and 8 dpi by RT-qPCR (**C**) (n = 3-7). **D.** Viral RNA *in situ* hybridization using SARS-CoV-2 probe (brown color) in the lungs harvested at 4 dpi. Images show low- (top; scale bars, 100 μm) and medium- (middle; scale bars, 100 μm) power magnification with a high-power magnification inset (representative images from n = 3 per group). **E.** Fold change in gene expression of indicated cytokines and chemokines from lung homogenates at 4 dpi was determined by RT-qPCR after normalization to *Gapdh* levels and comparison with naïve unvaccinated, unchallenged controls (n = 7). **F-G**. Mice that received a prime-boost immunization were challenged on day 35 post-booster immunization. Tissues were collected at 4 dpi for analysis. Infectious virus in the lung was determined by plaque assay (**F**) and viral RNA was measured in the lung, spleen and heart using RT-qPCR (**G**) (n = 6-7). (**B-C** and **E-G**) Columns show median values, and dotted lines indicate the LOD of the assays. For **B, C, E, F, and G**: Mann-Whitney test: *, $P < 0.05$; **, $P < 0.01$; ***, $P < 0.001$. **See Figure S3**.

Figure 3. Single-dose intramuscular vaccination with ChAd-SARS-CoV-2-S protects mice against SARS-CoV-2-induced inflammation in the lung. Four-week old female BALB/c mice were immunized with ChAd-control and ChAd-SARS-CoV-2-S and

challenged following the scheme described in **Figure 2**. Lungs were harvested at 8 dpi. Sections were stained with hematoxylin and eosin and imaged at 40x (left; scale bar, 250 μm), 200x (middle; scale, 50 μm), and 400x (right; scale bar, 25 μm) magnifications. Each image is representative of a group of 3 mice.

Figure 4. Immune responses after Intranasal immunization of ChAd-SARS-CoV-2-S. **A**. Scheme of experiments. Five-week-old BALB/c female mice were immunized with ChAd-control or ChAd-SARS-CoV-2-S via an intranasal route. (**B-D**) Antibody responses in sera of immunized mice at one month after priming were evaluated. An ELISA measured SARS-CoV-2 S-and RBD-specific IgG (**B**) and IgA levels (**C**), and a FRNT determined neutralization activity (**D**). Data are pooled from two experiments with n = 10-25 mice per group. **E-J.** Mice that received a booster dose were sacrificed one week later to evaluate mucosal and cell-mediated immune responses. SARS-CoV-2 S-and RBD-specific IgG (**E**) and IgA levels (**F**) in BAL fluid were determined by ELISA. Neutralizing activity of BAL fluid against SARS-CoV-2 was measured by FRNT (**G**). $CD8^+$ T cells in the lung were assayed for IFNγ and granzyme B expression by flow cytometry after re-stimulation with an S protein peptide pool (**H**). $CD8^+$ T cells in the lung also were phenotyped for expression of CD103 and CD69 (**I**). SARS-CoV-2 spike-specific IgG^+ and IgA^+ antibody-secreting cells (ASC) frequency in the spleen harvested one week post-boost was measured by ELISPOT (**J**). Data for mucosal and cell-mediated responses are pooled from two experiments (**E-I**: n = 7-9 per group; **J**: n = 5 per group). (**B-J**) Bars and columns show median values, and dotted lines indicate the LOD of the assays. Mann-Whitney test: **, $P < 0.01$; ***, $P < 0.001$; **** $P < 0.0001$. **See Figure S4 and Table S1.**

Figure 5. Single-dose intranasal immunization with ChAd-SARS-CoV-2-S protects against SARS-CoV-2 infection. Five-week-old BALB/c female mice were immunized with ChAd-control or ChAd-SARS-CoV-2-S via an intranasal route. On day 35 post-immunization, mice were challenged as follows: animals were treated with anti-Ifnar1 mAb and transduced with Hu-AdV5-hACE2 via the intranasal route one day later. Five days later, mice were

challenged intranasally with 4 x 10^5 FFU of SARS-CoV-2. (**A-C**) Tissues and nasal washes were collected at 4 and 8 dpi for analysis. Infectious virus in the lung was measured by plaque assay (**A**). Viral RNA levels in the lung, spleen, heart, nasal turbinates, and nasal washes were measured at 4 and 8 dpi by RT-qPCR (**B**). Fold change in gene expression of indicated cytokines and chemokines was determined by RT-qPCR, normalized to *Gapdh,* and compared to naïve controls in lung homogenates at 4 dpi (**C**) (2 experiments, n = 6-9; median values are shown). Columns show median values, and dotted lines indicate the LOD of the assays. **D**. Lungs were harvested at 8 dpi. Sections were stained with hematoxylin and eosin and imaged at 40x (left; scale bar, 250 μm), 200x (middle; scale, 50 μm), and 400x (right; scale bar, 25 μm) magnifications. Each image is representative of a group of 3 mice. **E**. An ELISA measured anti-SARS-CoV-2 NP IgM (*left*) and IgG (*right*) antibody responses in paired sera obtained 5 days before and 8 days after SARS-CoV-2 challenge of ChAd-control or ChAd-SARS-CoV-2-S mice vaccinated by an intranasal route (n = 6). Dotted lines represent the LOD of the assay. Dashed lines indicate the mark for a 4-fold increase of pre-boost IgM and IgG levels. For **A-C**: Mann-Whitney test: *, $P < 0.05$; **, $P < 0.01$; ***, $P < 0.001$; **** $P < 0.0001$; For **E**: ** $P < 0.01$, **** $P < 0.0001$, ns; not significant; paired t test). **See Figure S5.**

Figure 6. Immunogenicity and protective efficacy after Intranasal immunization of ChAd-SARS-CoV-2-S in K18-hACE2 mice. (**A**) Scheme of experiments. Four-week-old K18-hACE2 female mice were immunized with ChAd-control or ChAd-SARS-CoV-2-S via an intranasal route. (**B-D**) Antibody responses in sera of immunized mice at four weeks after priming were evaluated. An ELISA measured SARS-CoV-2 S-and RBD-specific IgG (**B**) and IgA levels (**C**), and a FRNT determined neutralization activity (**D**) (n = 7). (**E-G**) At one month post-immunization, mice were challenged with 10^3 FFU of SARS-CoV-2. Tissues and nasal washes were harvested at 4 dpi. Infectious virus in lungs was measured using plaque assay (**E**). Viral RNA levels in the lung, spleen, heart, nasal turbinates, and nasal washes were measured at 4 dpi by RT-qPCR (**F**). Fold change in gene expression of indicated cytokines and chemokines

was determined by RT-qPCR, normalized to *Gapdh,* and compared to naïve controls in lung homogenates at 4 dpi (**G**) (n = 7). Boxes indicate median values and dotted lines indicate the LOD of the assays. For **B-G**: Mann-Whitney test: **, $P < 0.01$; ***, $P < 0.001$. **See Figure S6.**

Figure 7. **Comparison of immunogenicity of single-dose administration of ChAd-SARS-CoV-2-S by intramuscular and intranasal delivery routes.** (*Upper panel*) After intramuscular inoculation, ChAd-SARS-CoV-2 vaccine transduces antigen-presenting cells (APCs) at the site of injection in muscle tissues. APCs migrate to lymphoid tissues where antigen-specific $CD8^+$T cells become activated, proliferate, and produce IFNγ and granzyme B. Antigen-specific B cells proliferate, some of which become plasmablasts and plasma cells that secrete anti-S IgG. After SARS-CoV-2 challenge, activated $CD8^+$ T cells migrate to the lungs to control infection and anti-S IgG neutralizes virus particles. Intramuscular vaccination protects against lower but not upper airway infection, and does not efficiently induce mucosal immunity. (*Lower panel*) After intranasal inoculation, ChAd-SARS-CoV-2 transduces APCs in the upper respiratory tract. APCs then migrate to bronchial or mucosal associated lymphoid tissues to present antigens to lymphocytes including B and T cells. After SARS-CoV-2 challenge, activated $CD8^+$ T cell migrate to the lungs, secrete cytokines, and attack virus-infected cells. Some $CD8^+$ T cells likely adopt a tissue resident memory phenotype ($CD103^+$ $CD69^+$) enabling them to reside in the lung (or upper airway) and respond more rapidly after re-encountering cognate antigen (SARS-CoV-2 S peptides). The activated B cell becomes response after intranasal vaccination produces cells that secrete anti-SARS-CoV-2-S IgG or IgA, the latter of which neutralizes virus within the upper and lower respiratory tracts. The mucosal immunity generated by intranasal inoculation of ChAd-SARS-CoV-2 likely controls infection at the point of initiation in the upper respiratory tract.

SUPPLEMENTARY FIGURE LEGENDS

578 **Figure S1. ChAd-SARS-CoV-2-S vaccine induces neutralizing antibodies as**
579 **measured by FRNT. Related to Figure 1.** Four-week old female BALB/c mice were primed or
580 primed and boosted with ChAd-control or ChAd-SARS-CoV-2-S via intramuscular route. **A-B**.
581 Serum samples from ChAd-control or ChAd-SARS-CoV-2 vaccinated mice were collected at
582 day 21 after priming (**A**) or boosting (**B**) and assayed for neutralizing activity by FRNT. Serum
583 neutralization curves corresponding to individual mice are shown for the indicated vaccines (n =
584 15-30 per group). Each point represents the mean of two technical replicates with error bars
585 denoting the standard deviations (SD). **C**. An ELISA measured anti-SARS-CoV-2 NP IgG
586 responses in paired sera obtained 5 days before and 8 days after SARS-CoV-2 challenge of
587 ChAd-control or ChAd-SARS-CoV-2-S mice vaccinated by an intramuscular route (n = 5: ** P <
588 0.01; *** P < 0.001; paired t test). Dotted lines represent the mean IgG titers from naïve sera.

589 **Figure S2. Gating strategy for analyzing T cell responses. Related to Figure 1**.
590 Four-week old female BALB/c mice were immunized with ChAd-control or ChAd-SARS-CoV-2-S
591 and boosted four weeks later. T cell responses were analyzed in splenocytes at day 7 post-
592 boost. Cells were gated for lymphocytes (FSC-A/SSC-A), singlets (SSC-W/SSC-H), live cells
593 ($Aqua^-$), $CD45^+$, $CD19^-$ followed by $CD4^+$ or $CD8^+$ cell populations expressing IFNγ or granzyme
594 B.

595 **Figure S3**. **Impact of pre-existing ChAd immunity on transduction of mice with Hu-**
596 **AdV5-hACE2. Related to Figures 1 and 2**. Four-week old female BALB/c mice were primed or
597 primed and boosted. Serum samples were collected one day prior to Hu-AdV5-hACE2
598 transduction. Neutralizing activity of Hu-AdV5-hACE2 in the sera from the indicated vaccine
599 groups was determined by FRNT after prime only (**A**) or prime and boost (**B**). Each symbol
600 represents a single animal; each point represents two technical repeats and bars indicate the
601 range. A positive control (anti-Hu-Adv5 serum) is included as a frame of reference.

602 **Figure S4. Intranasal inoculation of ChAd-SARS-CoV-2-S induces neutralizing**
603 **antibodies as measured by FRNT and protects against SARS-CoV-2 replication. Related**

to Figure 4 and Figure 5. Five-week old female BALB/c mice were immunized with ChAd-control or ChAd-SARS-CoV-2-S via an intranasal inoculation route. Serum samples collected one month after immunization were assayed for neutralizing activity by FRNT. Mice were boosted at day 30 after priming and were sacrificed one week later to evaluate immune responses. (**A**) Serum samples from ChAd-control or ChAd-SARS-CoV-2-S vaccinated mice were tested for neutralizing activity with SARS-CoV-2 strain 2019 n-CoV/USA_WA1/2020 (n = 8-10 per group). (**B**) Serum samples from ChAd-SARS-CoV-2-S vaccinated mice were tested for neutralization of recombinant luciferase-expressing SARS-CoV-2 viruses (wild-type (*left*) and D614G variant (*middle*)). (*Right*) Paired EC50 values are indicated (n = 5; n.s. not significant, paired t test). (**C**) BAL fluid was collected from ChAd-control or ChAd-SARS-CoV-2-S vaccinated mice, and neutralization of SARS-CoV-2 strain 2019 n-CoV/USA_WA1/2020 was measured using a FRNT assay (n = 8-10 per group). Each point represents the mean of two technical replicates with error bars denoting the SD. **D.** On day 35 post-immunization, mice were challenged via intranasal route with 4 x 10^5 FFU of SARS-CoV-2 five days after Hu-AdV5-hACE2 transduction and anti-Ifnar1 mAb treatment as described in **Figure 2**. Tissues were collected at 4 dpi for viral burden measurements. Genomic RNA (ORF1a) levels were determined in lungs and nasal turbinates (two experiments, n = 6-9; **** $P < 0.0001$; Mann-Whitney test). Columns show median values, and dotted lines indicate the LOD of the assays.

Figure S5. SARS-CoV-2 NP-specific IgM and IgG antibody responses following SARS-CoV-2 challenge. Related to Figure 5. Five-week-old BALB/c female mice were immunized with ChAd-control or ChAd-SARS-CoV-2-S via an intranasal route. One month later, mice were transduced with Hu-AdV5-ACE2 and challenged with SARS-CoV-2 as described in **Figure 5**. An ELISA measured anti-SARS-CoV-2 NP IgM and IgG responses in paired sera obtained 5 days before and 8 days after SARS-CoV-2 challenge. Serum ELISA curves corresponding to individual mice are shown for the indicated vaccines or control naïve BALB/c mice (n = 6 per group).

630 **Figure S6. Intranasal inoculation of ChAd-SARS-CoV-2-S induces neutralizing**
631 **antibodies in K18-hACE2 mice. Related to Figure 6.** Four-week old female K18-hACE2 mice
632 were immunized with ChAd-control or ChAd-SARS-CoV-2-S via an intranasal inoculation route.
633 Serum samples collected four weeks after immunization were assayed for neutralizing activity
634 by FRNT (n = 7 per group). Each point represents the mean of two technical replicates with
635 error bars denoting the SD.
636
637

REFERENCES

Abbink, P., Larocca, R.A., De La Barrera, R.A., Bricault, C.A., Moseley, E.T., Boyd, M., Kirilova, M., Li, Z., Ng'ang'a, D., Nanayakkara, O.*, et al.* (2016). Protective efficacy of multiple vaccine platforms against Zika virus challenge in rhesus monkeys. Science *353*, 1129-1132.

Alharbi, N.K., Qasim, I., Almasoud, A., Aljami, H.A., Alenazi, M.W., Alhafufi, A., Aldibasi, O.S., Hashem, A.M., Kasem, S., Albrahim, R.*, et al.* (2019). Humoral Immunogenicity and Efficacy of a Single Dose of ChAdOx1 MERS Vaccine Candidate in Dromedary Camels. Sci Rep *9*, 16292.

Alsoussi, W.B., Turner, J.S., Case, J.B., Zhao, H., Schmitz, A.J., Zhou, J.Q., Chen, R.E., Lei, T., Rizk, A.A., McIntire, K.M.*, et al.* (2020). A Potently Neutralizing Antibody Protects Mice against SARS-CoV-2 Infection. J Immunol.

Amanat, F., and Krammer, F. (2020). SARS-CoV-2 Vaccines: Status Report. Immunity *52*, 583-589.

Bolles, M., Deming, D., Long, K., Agnihothram, S., Whitmore, A., Ferris, M., Funkhouser, W., Gralinski, L., Totura, A., Heise, M.*, et al.* (2011). A double-inactivated severe acute respiratory syndrome coronavirus vaccine provides incomplete protection in mice and induces increased eosinophilic proinflammatory pulmonary response upon challenge. J Virol *85*, 12201-12215.

Burton, D.R., and Walker, L.M. (2020). Rational Vaccine Design in the Time of COVID-19. Cell Host Microbe *27*, 695-698.

Calzas, C., and Chevalier, C. (2019). Innovative Mucosal Vaccine Formulations Against Influenza A Virus Infections. Front Immunol *10*, 1605.

Cao, Y., Su, B., Guo, X., Sun, W., Deng, Y., Bao, L., Zhu, Q., Zhang, X., Zheng, Y., Geng, C.*, et al.* (2020). Potent neutralizing antibodies against SARS-CoV-2 identified by high-throughput single-cell sequencing of convalescent patients' B cells. Cell.

Case, J.B., Rothlauf, P.W., Chen, R.E., Liu, Z., Zhao, H., Kim, A., S., Bloyet, L.M., Zeng, Q., Tahan, S., Droit, L.*, et al.* (2020). Neutralizing antibody and soluble ACE2 inhibition of a replication-competent VSV-SARS-CoV-2 and a clinical isolate of SARS-CoV-2. Cell Host and Microbe, In press.

Chandrashekar, A., Liu, J., Martinot, A.J., McMahan, K., Mercado, N.B., Peter, L., Tostanoski, L.H., Yu, J., Maliga, Z., Nekorchuk, M.*, et al.* (2020). SARS-CoV-2 infection protects against rechallenge in rhesus macaques. Science.

Cheung, E.W., Zachariah, P., Gorelik, M., Boneparth, A., Kernie, S.G., Orange, J.S., and Milner, J.D. (2020). Multisystem Inflammatory Syndrome Related to COVID-19 in Previously Healthy Children and Adolescents in New York City. Jama.

Corbett, K.S., Flynn, B., Foulds, K.E., Francica, J.R., Boyoglu-Barnum, S., Werner, A.P., Flach, B., O'Connell, S., Bock, K.W., Minai, M.*, et al.* (2020). Evaluation of the mRNA-1273 Vaccine against SARS-CoV-2 in Nonhuman Primates. New England Journal of Medicine.

de Alwis, R., Chen, S., Gan, E.S., and Ooi, E.E. (2020). Impact of immune enhancement on Covid-19 polyclonal hyperimmune globulin therapy and vaccine development. EBioMedicine *55*, 102768.

de Wit, E., van Doremalen, N., Falzarano, D., and Munster, V.J. (2016). SARS and MERS: recent insights into emerging coronaviruses. Nat Rev Microbiol *14*, 523-534.

Diamond, M.S., and Pierson, T.C. (2020). The Challenges of Vaccine Development against a New Virus during a Pandemic. Cell Host Microbe *27*, 699-703.

Dicks, M.D., Spencer, A.J., Edwards, N.J., Wadell, G., Bojang, K., Gilbert, S.C., Hill, A.V., and Cottingham, M.G. (2012). A novel chimpanzee adenovirus vector with low human seroprevalence: improved systems for vector derivation and comparative immunogenicity. PloS one *7*, e40385.

Douglas, A.D., de Cassan, S.C., Dicks, M.D., Gilbert, S.C., Hill, A.V., and Draper, S.J. (2010). Tailoring subunit vaccine immunogenicity: maximizing antibody and T cell responses by using combinations of adenovirus, poxvirus and protein-adjuvant vaccines against Plasmodium falciparum MSP1. Vaccine *28*, 7167-7178.

Dutta, A., Huang, C.T., Lin, C.Y., Chen, T.C., Lin, Y.C., Chang, C.S., and He, Y.C. (2016). Sterilizing immunity to influenza virus infection requires local antigen-specific T cell response in the lungs. Sci Rep *6*, 32973.

Folegatti, P.M., Bittaye, M., Flaxman, A., Lopez, F.R., Bellamy, D., Kupke, A., Mair, C., Makinson, R., Sheridan, J., Rohde, C.*, et al.* (2020a). Safety and immunogenicity of a candidate Middle East respiratory syndrome coronavirus viral-vectored vaccine: a dose-escalation, open-label, non-randomised, uncontrolled, phase 1 trial. Lancet Infect Dis.

Folegatti, P.M., Ewer, K.J., Aley, P.K., Angus, B., Becker, S., Belij-Rammerstorfer, S., Bellamy, D., Bibi, S., Bittaye, M., Clutterbuck, E.A.*, et al.* (2020b). Safety and immunogenicity of the ChAdOx1 nCoV-19 vaccine against SARS-CoV-2: a preliminary report of a phase 1/2, single-blind, randomised controlled trial. The Lancet.

Gao, Q., Bao, L., Mao, H., Wang, L., Xu, K., Yang, M., Li, Y., Zhu, L., Wang, N., Lv, Z.*, et al.* (2020). Rapid development of an inactivated vaccine candidate for SARS-CoV-2. Science.

Graham, B.S. (2020). Rapid COVID-19 vaccine development. Science.

Grifoni, A., Weiskopf, D., Ramirez, S.I., Mateus, J., Dan, J.M., Moderbacher, C.R., Rawlings, S.A., Sutherland, A., Premkumar, L., Jadi, R.S.*, et al.* (2020). Targets of T Cell Responses to SARS-CoV-2 Coronavirus in Humans with COVID-19 Disease and Unexposed Individuals. Cell.

Guan, W.J., Ni, Z.Y., Hu, Y., Liang, W.H., Ou, C.Q., He, J.X., Liu, L., Shan, H., Lei, C.L., Hui, D.S.C.*, et al.* (2020). Clinical Characteristics of Coronavirus Disease 2019 in China. N Engl J Med.

Hashem, A.M., Algaissi, A., Agrawal, A.S., Al-Amri, S.S., Alhabbab, R.Y., Sohrab, S.S., A, S.A., Alharbi, N.K., Peng, B.H., Russell, M.*, et al.* (2019). A Highly Immunogenic, Protective, and Safe Adenovirus-Based Vaccine Expressing Middle East Respiratory Syndrome Coronavirus S1-

CD40L Fusion Protein in a Transgenic Human Dipeptidyl Peptidase 4 Mouse Model. J Infect Dis *220*, 1558-1567.

Hassan, A.O., Case, J.B., Winkler, E.S., Thackray, L.B., Kafai, N.M., Bailey, A.L., McCune, B.T., Fox, J.M., Chen, R.E., Alsoussi, W.B*., et al.* (2020). A SARS-CoV-2 Infection Model in Mice Demonstrates Protection by Neutralizing Antibodies. Cell.

Hassan, A.O., Dmitriev, I.P., Kashentseva, E.A., Zhao, H., Brough, D.E., Fremont, D.H., Curiel, D.T., and Diamond, M.S. (2019). A Gorilla Adenovirus-Based Vaccine against Zika Virus Induces Durable Immunity and Confers Protection in Pregnancy. Cell Rep *28*, 2634-2646.e2634.

He, T.C., Zhou, S., da Costa, L.T., Yu, J., Kinzler, K.W., and Vogelstein, B. (1998). A simplified system for generating recombinant adenoviruses. Proc Natl Acad Sci U S A *95*, 2509-2514.
Hillen, W., and Berens, C. (1994). Mechanisms underlying expression of Tn10 encoded tetracycline resistance. Annu Rev Microbiol *48*, 345-369.

Hodgson, S.H., Ewer, K.J., Bliss, C.M., Edwards, N.J., Rampling, T., Anagnostou, N.A., de Barra, E., Havelock, T., Bowyer, G., Poulton, I.D*., et al.* (2015). Evaluation of the efficacy of ChAd63-MVA vectored vaccines expressing circumsporozoite protein and ME-TRAP against controlled human malaria infection in malaria-naive individuals. J Infect Dis *211*, 1076-1086.

Hoffmann, M., Kleine-Weber, H., Schroeder, S., Kruger, N., Herrler, T., Erichsen, S., Schiergens, T.S., Herrler, G., Wu, N.H., Nitsche, A*., et al.* (2020). SARS-CoV-2 Cell Entry Depends on ACE2 and TMPRSS2 and Is Blocked by a Clinically Proven Protease Inhibitor. Cell.

Kobinger, G.P., Figueredo, J.M., Rowe, T., Zhi, Y., Gao, G., Sanmiguel, J.C., Bell, P., Wivel, N.A., Zitzow, L.A., Flieder, D.B*., et al.* (2007). Adenovirus-based vaccine prevents pneumonia in ferrets challenged with the SARS coronavirus and stimulates robust immune responses in macaques. Vaccine *25*, 5220-5231.

Korber, B., Fischer, W.M., Gnanakaran, S., Yoon, H., Theiler, J., Abfalterer, W., Hengartner, N., Giorgi, E.E., Bhattacharya, T., Foley, B*., et al.* (2020). Tracking Changes in SARS-CoV-2 Spike: Evidence that D614G Increases Infectivity of the COVID-19 Virus. Cell.

Laurie, K.L., Carolan, L.A., Middleton, D., Lowther, S., Kelso, A., and Barr, I.G. (2010). Multiple infections with seasonal influenza A virus induce cross-protective immunity against A(H1N1) pandemic influenza virus in a ferret model. J Infect Dis *202*, 1011-1020.

Letko, M., Marzi, A., and Munster, V. (2020). Functional assessment of cell entry and receptor usage for SARS-CoV-2 and other lineage B betacoronaviruses. Nature microbiology *5*, 562-569.

Liu, L., Wei, Q., Lin, Q., Fang, J., Wang, H., Kwok, H., Tang, H., Nishiura, K., Peng, J., Tan, Z*., et al.* (2019). Anti-spike IgG causes severe acute lung injury by skewing macrophage responses during acute SARS-CoV infection. JCI insight *4*.

López-Camacho, C., Abbink, P., Larocca, R.A., Dejnirattisai, W., Boyd, M., Badamchi-Zadeh, A., Wallace, Z.R., Doig, J., Velazquez, R.S., Neto, R.D.L*., et al.* (2018). Rational Zika vaccine design via the modulation of antigen membrane anchors in chimpanzee adenoviral vectors. Nat Commun *9*, 2441.

Maizel, J.V., Jr., White, D.O., and Scharff, M.D. (1968). The polypeptides of adenovirus. I. Evidence for multiple protein components in the virion and a comparison of types 2, 7A, and 12. Virology *36*, 115-125.

Mao, R., Qiu, Y., He, J.S., Tan, J.Y., Li, X.H., Liang, J., Shen, J., Zhu, L.R., Chen, Y., Iacucci, M.*, et al.* (2020). Manifestations and prognosis of gastrointestinal and liver involvement in patients with COVID-19: a systematic review and meta-analysis. The lancet Gastroenterology & hepatology.

McCray, P.B., Jr., Pewe, L., Wohlford-Lenane, C., Hickey, M., Manzel, L., Shi, L., Netland, J., Jia, H.P., Halabi, C., Sigmund, C.D.*, et al.* (2007). Lethal infection of K18-hACE2 mice infected with severe acute respiratory syndrome coronavirus. J Virol *81*, 813-821.

Munster, V.J., Feldmann, F., Williamson, B.N., van Doremalen, N., Pérez-Pérez, L., Schulz, J., Meade-White, K., Okumura, A., Callison, J., Brumbaugh, B.*, et al.* (2020). Respiratory disease in rhesus macaques inoculated with SARS-CoV-2. Nature.

Munster, V.J., Wells, D., Lambe, T., Wright, D., Fischer, R.J., Bushmaker, T., Saturday, G., van Doremalen, N., Gilbert, S.C., de Wit, E.*, et al.* (2017). Protective efficacy of a novel simian adenovirus vaccine against lethal MERS-CoV challenge in a transgenic human DPP4 mouse model. NPJ Vaccines *2*, 28.

Neutra, M.R., and Kozlowski, P.A. (2006). Mucosal vaccines: the promise and the challenge. Nat Rev Immunol *6*, 148-158.

Ni, L., Ye, F., Cheng, M.L., Feng, Y., Deng, Y.Q., Zhao, H., Wei, P., Ge, J., Gou, M., Li, X.*, et al.* (2020). Detection of SARS-CoV-2-Specific Humoral and Cellular Immunity in COVID-19 Convalescent Individuals. Immunity *52*, 971-977.e973.

Pallesen, J., Wang, N., Corbett, K.S., Wrapp, D., Kirchdoerfer, R.N., Turner, H.L., Cottrell, C.A., Becker, M.M., Wang, L., Shi, W.*, et al.* (2017). Immunogenicity and structures of a rationally designed prefusion MERS-CoV spike antigen. Proc Natl Acad Sci U S A *114*, E7348-e7357.

Penaloza-MacMaster, P., Provine, N.M., Ra, J., Borducchi, E.N., McNally, A., Simmons, N.L., Iampietro, M.J., and Barouch, D.H. (2013). Alternative serotype adenovirus vaccine vectors elicit memory T cells with enhanced anamnestic capacity compared to Ad5 vectors. J Virol *87*, 1373-1384.

Pinto, D., Park, Y.J., Beltramello, M., Walls, A.C., Tortorici, M.A., Bianchi, S., Jaconi, S., Culap, K., Zatta, F., De Marco, A.*, et al.* (2020). Cross-neutralization of SARS-CoV-2 by a human monoclonal SARS-CoV antibody. Nature.

Rathnasinghe, R., Strohmeier, S., Amanat, F., Gillespie, V.L., Krammer, F., García-Sastre, A., Coughlan, L., Schotsaert, M., and Uccellini, M. (2020). Comparison of Transgenic and Adenovirus hACE2 Mouse Models for SARS-CoV-2 Infection. bioRxiv.

Reyes-Sandoval, A., Berthoud, T., Alder, N., Siani, L., Gilbert, S.C., Nicosia, A., Colloca, S., Cortese, R., and Hill, A.V. (2010). Prime-boost immunization with adenoviral and modified vaccinia virus Ankara vectors enhances the durability and polyfunctionality of protective malaria CD8+ T-cell responses. Infect Immun *78*, 145-153.

Roy, S., Medina-Jaszek, A., Wilson, M.J., Sandhu, A., Calcedo, R., Lin, J., and Wilson, J.M. (2011). Creation of a panel of vectors based on ape adenovirus isolates. J Gene Med *13*, 17-25.

Sabo, M.C., Luca, V.C., Prentoe, J., Hopcraft, S.E., Blight, K.J., Yi, M., Lemon, S.M., Ball, J.K., Bukh, J., Evans, M.J.*, et al.* (2011). Neutralizing Monoclonal Antibodies against Hepatitis C Virus E2 Protein Bind Discontinuous Epitopes and Inhibit Infection at a Postattachment Step. J Virol *85*, 7005-7019.

Sheehan, K.C., Lai, K.S., Dunn, G.P., Bruce, A.T., Diamond, M.S., Heutel, J.D., Dungo-Arthur, C., Carrero, J.A., White, J.M., Hertzog, P.J.*, et al.* (2006). Blocking monoclonal antibodies specific for mouse IFN-alpha/beta receptor subunit 1 (IFNAR-1) from mice immunized by in vivo hydrodynamic transfection. J Interferon Cytokine Res *26*, 804-819.

Slifka, M.K., and Amanna, I. (2014). How advances in immunology provide insight into improving vaccine efficacy. Vaccine *32*, 2948-2957.

Takamura, S. (2017). Persistence in Temporary Lung Niches: A Survival Strategy of Lung-Resident Memory CD8(+) T Cells. Viral Immunol *30*, 438-450.

Weingartl, H., Czub, M., Czub, S., Neufeld, J., Marszal, P., Gren, J., Smith, G., Jones, S., Proulx, R., Deschambault, Y.*, et al.* (2004). Immunization with modified vaccinia virus Ankara-based recombinant vaccine against severe acute respiratory syndrome is associated with enhanced hepatitis in ferrets. J Virol *78*, 12672-12676.

Wichmann, D., Sperhake, J.P., Lütgehetmann, M., Steurer, S., Edler, C., Heinemann, A., Heinrich, F., Mushumba, H., Kniep, I., Schröder, A.S.*, et al.* (2020). Autopsy Findings and Venous Thromboembolism in Patients With COVID-19: A Prospective Cohort Study. Ann Intern Med.

Winkler, E.S., Bailey, A.L., Kafai, N.M., Nair, S., McCune, B.T., Yu, J., Fox, J.M., Chen, R.E., Earnest, J.T., Keeler, S.P.*, et al.* (2020). SARS-CoV-2 infection in the lungs of human ACE2 transgenic mice causes severe inflammation, immune cell infiltration, and compromised respiratory function. bioRxiv

Wrapp, D., Wang, N., Corbett, K.S., Goldsmith, J.A., Hsieh, C.L., Abiona, O., Graham, B.S., and McLellan, J.S. (2020). Cryo-EM structure of the 2019-nCoV spike in the prefusion conformation. Science.

Yu, J., Tostanoski, L.H., Peter, L., Mercado, N.B., McMahan, K., Mahrokhian, S.H., Nkolola, J.P., Liu, J., Li, Z., Chandrashekar, A.*, et al.* (2020). DNA vaccine protection against SARS-CoV-2 in rhesus macaques. Science.

Yuan, M., Wu, N.C., Zhu, X., Lee, C.D., So, R.T.Y., Lv, H., Mok, C.K.P., and Wilson, I.A. (2020). A highly conserved cryptic epitope in the receptor-binding domains of SARS-CoV-2 and SARS-CoV. Science.

Yusuf, H., and Kett, V. (2017). Current prospects and future challenges for nasal vaccine delivery. Human vaccines & immunotherapeutics *13*, 34-45.

Zhou, F., Yu, T., Du, R., Fan, G., Liu, Y., Liu, Z., Xiang, J., Wang, Y., Song, B., Gu, X.*, et al.* (2020a). Clinical course and risk factors for mortality of adult inpatients with COVID-19 in Wuhan, China: a retrospective cohort study. Lancet *395*, 1054-1062.

Zhou, P., Yang, X.L., Wang, X.G., Hu, B., Zhang, L., Zhang, W., Si, H.R., Zhu, Y., Li, B., Huang, C.L.*, et al.* (2020b). A pneumonia outbreak associated with a new coronavirus of probable bat origin. Nature *579*, 270-273.

Zhu, F.C., Li, Y.H., Guan, X.H., Hou, L.H., Wang, W.J., Li, J.X., Wu, S.P., Wang, B.S., Wang, Z., Wang, L.*, et al.* (2020). Safety, tolerability, and immunogenicity of a recombinant adenovirus type-5 vectored COVID-19 vaccine: a dose-escalation, open-label, non-randomised, first-in-human trial. Lancet *395*, 1845-1854.

Zost, S.J., Gilchuk, P., Chen, R.E., Case, J.B., Reidy, J.X., Trivette, A., Nargi, R.S., Sutton, R.E., Suryadevara, N., Chen, E.C.*, et al.* (2020). Rapid isolation and profiling of a diverse panel of human monoclonal antibodies targeting the SARS-CoV-2 spike protein. Nat Med.

Highlights

- Chimpanzee adenoviral vaccines encoding stabilized S induce neutralizing Abs
- Chimpanzee adenoviral vaccines protect against SARS-CoV-2 infection and pneumonia
- Intranasal vaccine delivery generates robust mucosal B and T cell responses
- Intranasal ChAd-SARS-CoV-2 prevents upper and low respiratory tract infection

eTOC Blurb

Intranasal or intramuscular immunization of ChAd-SARS-CoV-2, a chimpanzee adenoviral vaccine encoding stabilized spike intramuscular prevents SARS-CoV-2 lung infection and pneumonia in mice. In particular, intranasally delivered ChAd-SARS-CoV-2 uniquely prevents both upper and lower respiratory tract infections, potentially protecting against SARS-CoV-2 infection and transmission.

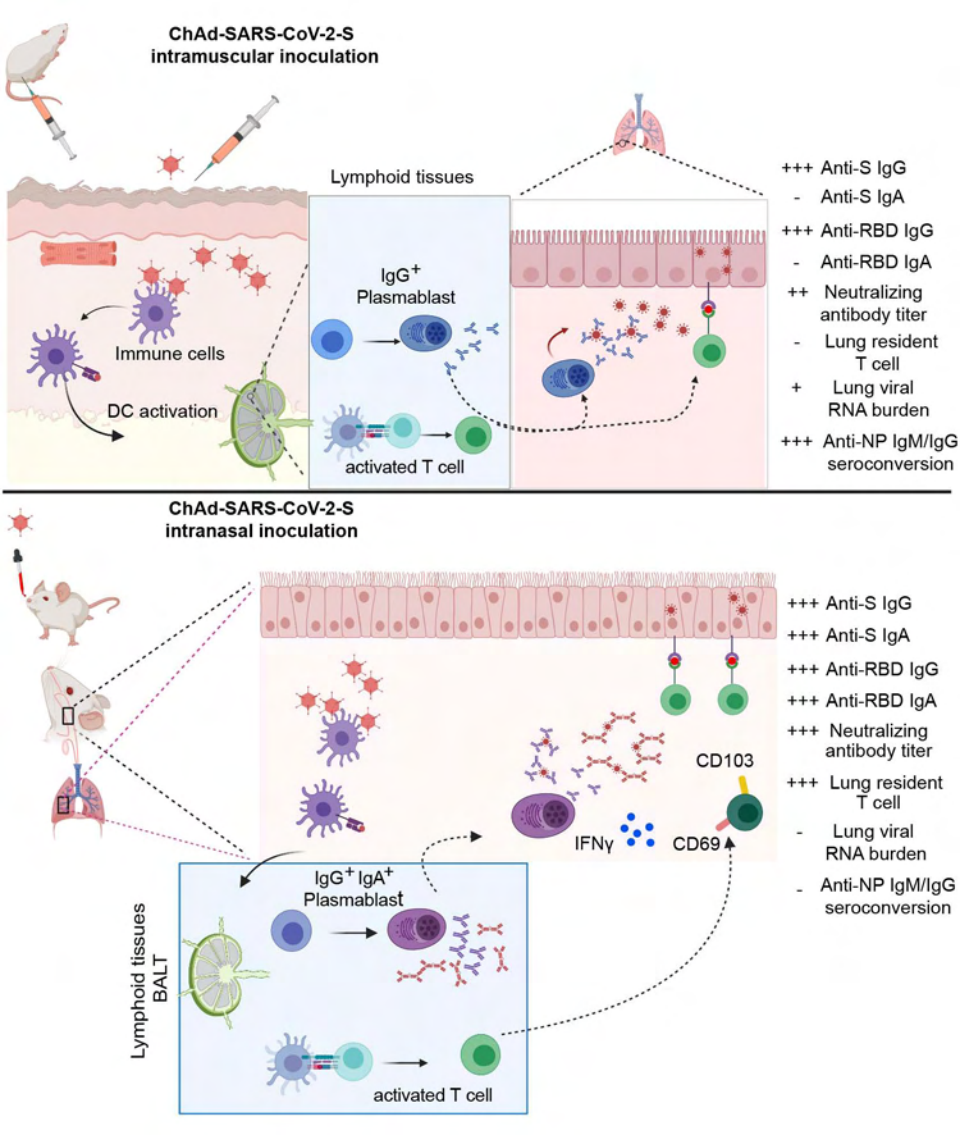
ChAd-SARS-CoV-2-S
intramuscular inoculation
Lymphoid tissues
IgG+
Plasmablast
Immune cells
DC activation
activated T cell
+++ Anti-S IgG
- Anti-S IgA
+++ Anti-RBD IgG
- Anti-RBD IgA
++ Neutralizing antibody titer
- Lung resident T cell
+ Lung viral RNA burden
+++ Anti-NP IgM/IgG seroconversion
ChAd-SARS-CoV-2-S
intranasal inoculation
+++ Anti-S IgG
+++ Anti-S IgA
+++ Anti-RBD IgG
+++ Anti-RBD IgA
+++ Neutralizing antibody titer
+++ Lung resident T cell
- Lung viral RNA burden
- Anti-NP IgM/IgG seroconversion
CD103
IFNγ
CD69
IgG+ IgA+
Plasmablast
Lymphoid tissues
BALT
activated T cell